chemosensors

MDPI

Article

Discovery of Lithospermate B as a Potential Ligand for the Malarial E2 Ubiquitin-Conjugating Enzyme via Multiplexed Native Mass Spectrometry

Jianying Han [1,2], Wesley C. Van Voorhis [3], Ronald J. Quinn [1] and Miaomiao Liu [1,*]

[1] Institute for Biomedicine and Glycomics, Griffith University, Brisbane, QLD 4111, Australia; jianying.han@uq.edu.au (J.H.); r.quinn@griffith.edu.au (R.J.Q.)
[2] Institute for Molecular Bioscience, The University of Queensland, St Lucia, QLD 4072, Australia
[3] Center for Emerging and Re-emerging Infectious Diseases, Department of Medicine, University of Washington School of Medicine, MS 358061, 750 Republican St., Seattle, WA 98109-4766, USA; wvanvoorhis@medicine.washington.edu
* Correspondence: miaomiao.liu@griffith.edu.au; Tel.: +61-7-3735-4412

Abstract: There is an urgent need for novel therapeutics to combat *Plasmodium falciparum*, especially in light of increasing drug resistance. Here, we present a multiplexed native mass spectrometry (MS) platform capable of simultaneously screening multiple protein targets against chemically diverse crude extracts with minimal sample preparation. A mixture of seven malarial proteins was analyzed under optimized native MS conditions, enabling the detection of specific ligand binding events. Using this platform, lithospermate B from *Salvia miltiorrhiza* (Danshen) was identified as a novel ligand for a malarial ubiquitin-conjugating enzyme with moderate affinity (Kd = 30.5 ± 2.5 μM). This is the first report linking lithospermate B to a malarial protein target, highlighting the potential of native MS to uncover new bioactivities of known natural products. This approach significantly enhances the throughput of protein–ligand screening and offers a powerful tool for early-stage natural product-based drug discovery.

Keywords: native mass spectrometry; lithospermate B; ubiquitin-conjugating enzyme; *Salvia miltiorrhiza*

check for updates

Received: 31 March 2025
Revised: 29 April 2025
Accepted: 1 May 2025
Published: 5 May 2025

Citation: Han, J.; Van Voorhis, W.C.; Quinn, R.J.; Liu, M. Discovery of Lithospermate B as a Potential Ligand for the Malarial E2 Ubiquitin-Conjugating Enzyme via Multiplexed Native Mass Spectrometry. *Chemosensors* **2025**, *13*, 166. https://doi.org/10.3390/chemosensors13050166

Copyright: © 2025 by the authors. Licensee MDPI, Basel, Switzerland. This article is an open access article distributed under the terms and conditions of the Creative Commons Attribution (CC BY) license (https://creativecommons.org/licenses/by/4.0/).

1. Introduction

Malaria remains one of the most devastating infectious diseases worldwide, with *Plasmodium falciparum* being the most lethal malaria parasite [1]. The emergence of drug-resistant strains has underscored the urgent need for novel therapeutic strategies and the identification of new drug targets [2]. Natural products have historically been a rich source of bioactive compounds, and their potential to interact with malarial proteins offers a promising avenue for drug discovery [3]. However, studying protein–ligand interactions within complex natural product extracts remains highly challenging due to their chemical complexity, low yields of active constituents, and the labor-intensive requirement for pre-purification. These challenges highlight the need for an analytical technique capable of precisely characterizing protein–ligand interactions with high sensitivity and resolution without the need for extensive sample preparation.

Native mass spectrometry (native MS) has emerged as a powerful analytical technique for studying intact protein complexes and their interactions with ligands under near-native conditions [4]. Compared to conventional methods such as surface plasmon resonance (SPR) [5], isothermal titration calorimetry (ITC) [6], and thermal shift assays (TSA) [7],

this native MS-based screening technique offers several distinct advantages. First, it is label-free, eliminating the need for chemical modifications that may interfere with binding. Second, it preserves the native conformation of proteins in the gas phase, allowing for the detection of transient or weak interactions that might be missed using other techniques. Third, native MS provides immediate mass-based identification of ligands, enabling rapid identification and downstream structural analysis. Finally, in the context of natural product research, native MS is uniquely suited to handle chemically complex samples with minimal sample preparation.

A typical native MS spectrum often displays multiple charge states (z), where fewer charge states and lower charge states indicate that the protein is in its native state. Native MS preserves non-covalent interactions, allowing for the direct detection of protein–ligand complexes [8]. This technique is particularly well-suited for screening natural product extracts, as it allows for the accurate identification of potential ligands by directly providing their molecular weight, calculated as [m/z (protein–ligand complex) $-$ m/z (protein)] $\times$ z [9]. By maintaining the native state of the protein, native MS provides insights into the stoichiometry, specificity, and stability of protein–ligand interactions, which are critical for understanding the molecular mechanisms underlying ligand binding [10].

With its high speed, sensitivity, and resolution, native MS has been widely applied in library screenings to discover ligands binding to proteins [11,12]. Successful applications include screenings of pure compound libraries [13,14], natural product fragment libraries [15,16], and natural product fraction mixtures [17]. In this study, we leverage the high resolution and sensitivity of native MS to investigate a mixture of seven malarial proteins against natural product extracts. This advancement allows for the simultaneous identification of potential ligands across multiple protein targets, significantly enhancing screening efficiency. By analyzing protein–ligand interactions in a multiplexed format, the platform not only reduces the time and resources required for screening but also provides a more comprehensive understanding of the binding preferences and specificities of natural product ligands.

2. Materials and Methods

2.1. General Experimental Procedures

Nuclear magnetic resonance (NMR) spectra were acquired at 25 °C using a Bruker Avance HDX 800 MHz spectrometer equipped with a TCI cryoprobe (Bruker, Billerica, MA, USA), with chemical shifts referenced to residual DMSO-d_6 signals (δ_H 2.50 and δ_C 39.5).

Targeted isolation of the natural product was guided by LC-MS analysis, performed on an Ultimate 3000RS UHPLC system coupled to a Thermo Fisher Scientific MSQ Plus ESI single quadrupole mass spectrometer.

High-resolution mass spectrometry (HRMS) data for compound characterization were obtained using a Bruker maXis II ETD ESI-qTOF instrument (Bruker, Billerica, MA, USA).

Extraction steps were conducted using an Edwards Instrument Company Bioline orbital shaker.

Preparative and semi-preparative HPLC separations were carried out on a Thermo Ultimate 3000 system equipped with a photodiode array (PDA) detector (Thermo Fisher Scientific, Waltham, MA, USA).

Analytical HPLC was performed using a Phenomenex C18 Monolithic column (5 µm, 4.6 × 100 mm), while semi-preparative purification employed Thermo Hypersil Gold C18 (5 µm, 10 × 250 mm) and Phenomenex Luna C18 (5 µm, 10 × 250 mm) columns.

Optical rotation measurements were recorded on a JASCO P-1020 polarimeter with a 10 cm cell (JASCO, Tokyo, Japan).

All solvents used in extraction, chromatography, optical rotation, and mass spectrometry were of HPLC grade, and water was purified using a Milli-Q system (Millipore, Rahway, NJ, USA).

2.2. Malarial Proteins

Seven *P. falciparum* proteins were expressed in *Escherichia coli* following previously described procedures [18,19].

2.3. TCM Materials

Six TCMs, Huangqi (*Astragalus mongholicus*), Danshen (*Salvia miltiorrhiza*), Wuweizi (*Schisandra chinensis*), Baibu (*Stemona tuberosa*), Tiandong (*Asparagus cochinchinensis*), and Daji (*Cirsium japonicum*), were purchased from a Chinese medicine clinic in Brisbane, Australia (Beijing Tong Ren Tang Australia–Brisbane store).

2.4. Extraction of the TCMs

The ground and freeze-dried TCMs (10 g each) were extracted with 95% ethanol (3 × 300 mL) overnight at room temperature to obtain crude extracts. The resulting crude extract yields were as follows: 1.45 g (Huangqi), 0.95 g (Danshen), 4.5 g (Wuweizi), 4.22 g (Baibu), 1.53 g (Tiandong), and 0.98 g (Daji).

2.5. Compound Isolation from Danshen

A total of 0.95 g of crude *Danshen* extract was fractionated using a Sephadex LH-20 column (column volume: 200 mL). Sixty fractions (Fractions 1–60) were collected by eluting with 100% methanol, with each fraction containing 10 mL of eluate. Every set of five consecutive fractions was pooled and analyzed by LC-MS to identify pools containing the target ligand with a molecular weight of 718 Da. Individual fractions within the identified pools were subsequently analyzed by LC-MS to validate the presence of the target ligand. Based on LC-MS and ^{1}H NMR profiles, fractions containing the target compound were combined and further purified by HPLC.

2.6. Protein Preparation

For individual protein experiments, each protein was buffer-exchanged into 50 mM ammonium acetate (pH 7.3) using size exclusion chromatography (Nalgene NAP-5, G25, GE Healthcare, Waukesha, WI, USA) prior to native MS analysis. The final concentration of each protein was 10 μM.

For protein mixture experiments, the seven proteins were first mixed and then buffer-exchanged into ammonium acetate at selected concentrations (10 mM, 50 mM, 100 mM, or 200 mM) prior to native MS analysis. The final concentration of each protein in the mixture was 5 μM.

Each TCM crude extract was dissolved in methanol at a concentration of 100 mg/mL. For screening assays, 1 μL of crude extract was incubated with 49 μL of the protein mixture for 1 h at room temperature, resulting in a final crude extract concentration of 2 mg/mL in the assay. Samples were then analyzed by native MS under the conditions described below.

2.7. Mass Spectrometry Instrument Control and Acquisition

All native MS experiments were performed on a Bruker SolariX XR 12T Fourier transform ion cyclotron resonance (FT-ICR) mass spectrometer (Bruker Daltonics Inc., Billerica, MA, USA). The ESI source was operated in direct injection mode using a 500 μL Hamilton syringe on the built-in syringe pump at a flow rate of 120 μL/h. The capillary voltage was set to 4000 V, and the end-plate offset voltage was set to −500 V. The dry gas flow rate was maintained at 4 L/min, and the dry gas temperature was 200 °C.

The source optics voltages were set as follows: capillary exit, 200 V; deflector plate, 220 V; funnel 1, 150 V; and skimmer 1, 30 V. Mass spectra were acquired in positive ion mode using profile acquisition across an m/z range of 50–6000. Each spectrum was generated by summing 16 transients (scans), with each transient composed of 1 million data points. All pulse sequence control and data acquisition were managed using Solarix control software (DataAnalysis Version 5.2) running under a Windows operating system.

2.8. Lithospermate B

Yellow powder, $[\alpha]_D^{25}$ +28 (*c* 0.4, MeOH); ^{1}H NMR (800 MHz, DMSO-d_6) δ_H 7.43 (1H, d, *J* = 15.8 Hz, H-25), 7.22 (1H, d, *J* = 8.5 Hz, H-5), 6.82 (1H, d, *J* = 8.5 Hz, H-6), 6.74 (1H, d, *J* = 2.0 Hz, H-32), 6.73 (1H, d, *J* = 8.0 Hz, H-11), 6.70 (1H, d, *J* = 2.0 Hz, H-14), 6.56 (1H, d, *J* = 2.0 Hz, H-20), 6.55 (1H, dd, *J* = 8.5, 2.0 Hz, H-10), 6.54 (1H, d, *J* = 8.0 Hz, H-23), 6.49 (1H, dd, *J* = 8.0, 2.0 Hz, H-24), 6.29 (1H, dd, *J* = 8.0, 2.0 Hz, H-36), 6.25 (1H, d, *J* = 15.8 Hz, H-26), 6.60 (1H, d, *J* = 8.0 Hz, H-35), 5.65 (1H, d, *J* = 4.5 Hz, H-1), 5.00 (1H, dd, *J* = 9.4, 3.8 Hz, H-16), 4.97 (1H, dd, *J* = 8.8, 4.1 Hz, H-28), 4.35 (1H, d, *J* = 4.5 Hz, H-2), 2.95 (1H, m, H-18a), 2.95 (1H, m, H-30a), 2.87 (1H, dd, *J* = 14.4, 8.8 Hz, H-30b), 2.77 (1H, dd, *J* = 14.4, 9.4 Hz, H-18b); ^{13}C NMR data (200 MHz, DMSO-d_6) δ_C 171.5 (C, C-29), 170.8 (C, C-17), 170.4 (C, C-15), 165.9 (C, C-27), 147.3 (C, C-8), 145.7 (C, C-12), 145.5 (C, C-13), 145.1 (C, C-33), 145.0 (C, C-34), 144.0 (C, C-22), 143.9 (C, C-7), 143.9 (C, C-21), 141.6 (CH, C-25), 131.4 (C, C-9), 128.1 (C, C-31), 127.8 (C, C-19), 125.0 (C, C-3), 122.8 (C, C-4), 121.2 (CH, C-5), 119.9 (C, C-36). 119.9 (CH, C-24), 117.3 (CH, C-6), 117.0 (CH, C-10), 116.9 (CH, C-32), 116.5 (CH, C-20), 116.0 (CH, C-26), 115.6 (CH, C-23), 115.6 (CH, C-11), 115.4 (CH, C-35), 112.6 (CH, C-14), 86.1 (CH, C-1), 75.0 (CH, C-16), 74.2 (CH, C-28), 55.6 (CH, C-2), 36.5 (CH_2, C-30), 36.3 (CH_2, C-18), HRMS *m/z* 717.1463 $[M-H]^-$, calcd. for $C_{36}H_{29}O_{16}^-$, 717.1461.

2.9. Kd Determination

Lithospermate B solutions were prepared in DMSO through serial dilutions to achieve the following concentrations: 0.1, 0.3, 1, 3, 10, 30, 100, 200, and 300 µM. For each concentration, 1 µL was added to individual wells of a V-bottom microtiter plate (BioCentrix, Carlsbad, CA, USA). DMSO was removed from each well using a freeze dryer (Christ, Osterode am Harz, Germany), followed by the addition of 1 µL of methanol.

The ubiquitin-conjugating enzyme was buffer-exchanged into 50 mM ammonium acetate (pH 7.3) using a Nalgene NAP-5 size exclusion column prior to native MS analysis. Subsequently, 49 µL of protein solution was added to each well containing lithospermate B. Samples were incubated for 60 min at room temperature, and then directly infused into the mass spectrometer using electrospray ionization (ESI). All experiments were performed in triplicate.

The relative abundances of the protein–ligand complex compared to the total protein in the mass spectra were used to determine the equilibrium binding. The dissociation constant (Kd) was calculated using the following equations:

$$\frac{\sum I(P-L)^{n+}/n}{\sum I(P)^{n+}/n+\sum I(P-L)^{n+}/n}=\frac{[P-L]}{[P]_t} \quad (1)$$

$$\frac{\sum I(P-L)^{n+}/n}{\sum I(P)^{n+}/n+\sum I(P-L)^{n+}/n}=\frac{[P]_t+[L]_t+Kd-\sqrt{([P]_t+[L]_t+Kd)^2-4[P]_t[L]_t}}{2[P]_t} \quad (2)$$

where $[P-L]^{n+}$ is the intensity of the protein−ligand complex at charge state n, and $[P]^{n+}$ is the intensity of the apo-protein at charge state n. Summation was performed across all observed charge states [20]. A binding curve was generated by plotting the ligand concentration against the percentage of ligand-bound protein, and the Kd was

determined by fitting the data using non-linear regression in GraphPad Prism 10.2.0, according to the equation:

$$Y = Bmax \times X/(K_d + X) \quad (3)$$

3. Results

3.1. Malarial Proteins

In this study, we selected seven malarial proteins as targets for ligand discovery using native mass spectrometry (MS). These proteins were chosen based on their essential roles in the *Plasmodium* life cycle and their potential as drug targets. The selected proteins include adenosine deaminase (ADA, PVX_111245), dUTPase (PF3D7_1127100), eukaryotic translation initiation factor 5A (eIF5A, PF3D7_1204300), tryptophan tRNA ligase (PF3D7_1336900), ubiquitin carboxyl-terminal hydrolase (PF3D7_1460400), ubiquitin conjugating enzyme (PF3D7_1203900), and HU homolog (PF3D7_0904700).

Adenosine deaminase (ADA) plays a key role in purine metabolism, a pathway essential for parasite survival, as *Plasmodium* species lack the ability to synthesize purines de novo and must rely on purine salvage [21]. Inhibitors of ADA have demonstrated antimalarial potential, highlighting this enzyme as a promising target for antimalarial drug discovery [22]. Protein dUTPase is essential in both eukaryotes and prokaryotes, playing a critical role in nucleotide metabolism by preventing the misincorporation of uracil into DNA, an essential process for parasite replication [23]. The *Pf* dUTPase shares relatively low sequence identity (28.4%) with its human ortholog, making it an attractive target for selective drug development [24]. Several inhibitors of *Pf* dUTPase have been reported to exhibit antimalarial activity, further supporting its potential as a therapeutic target [25]. Protein eIF5A is conserved across all three kingdoms and is involved in post-translational protein modification through the formation of hypusine, a unique amino acid critical for its function [26]. Although the exact mechanism of eIF5A activity is not fully understood, it has been shown to be essential for cell proliferation and apoptosis, highlighting its potential as a drug target [27]. Tryptophan tRNA ligase is a member of the minoacyl-tRNA synthetases (aaRSs), which have been proven as potent antimalarial drug targets owing to their pivotal role in protein synthesis [28]. The inhibition of this protein results in the decimation of protein synthesis and subsequent cell death [29]. Ubiquitin carboxyl-terminal hydrolase and ubiquitin-conjugating enzyme are key players in the parasite's ubiquitin-proteasome system, which is vital for protein degradation and parasite development [30]. Small molecular inhibitors of the UPS system in malaria demonstrated their high efficacy against asexual P. falciparum blood stages [31,32]. HU homolog is a DNA-binding protein implicated in nucleoid organization, potentially influencing gene expression and replication in Plasmodium [33].

These targets were selected not only for their biological significance but also for their diverse biochemical properties, making them ideal candidates for a broad-spectrum ligand screening approach.

3.2. Native Mass Spectrometry Platform

Native MS has been widely applied to study protein–ligand interactions in various contexts, with most applications focusing on individual proteins tested against ligands of varying complexity. By integrating a fast size exclusion chromatography step, native MS has been adapted to rapidly identify ligands from complex natural product extracts that bind to a single protein [34]. Its high sensitivity enables the detection of weak-binding ligands even at low concentrations within complex mixtures, while its high resolution allows for effective differentiation between ligands with closely related masses.

Building on a previous study in which a mixture of five proteins ranging from 12 to 42 kDa was successfully analyzed simultaneously for ligand binding under various instrument conditions [35], this work seeks to extend the native MS screening platform to accommodate a larger set of proteins for simultaneous screening.

The selected seven malarial proteins were individually analyzed by native MS to assess their ionization and native-state conformations (Figure 1). At a concentration of 10 μM, each protein exhibited characteristic native MS spectra, displaying narrow charge state distributions, consistent with folded conformations in the gas phase. Specifically, ADA showed a dominant charge state of 12+ (*m/z* 3569), with minor species at 13+ (*m/z* 3295) and 11+ (*m/z* 3894), corresponding to a calculated molecular weight (MW) of 42,824 Da. Protein dUTPase exhibited a major 8+ charge state (*m/z* 2543), along with 7+ (*m/z* 2906) and 9+ (*m/z* 2268), yielding a MW of 20,334 Da. The eIF5A showed a primary 8+ charge state (*m/z* 2317), with additional peaks at 7+ (*m/z* 2647) and 9+ (*m/z* 2059), corresponding to a MW of 18,524 Da. Tryptophan tRNA ligase presented a dominant 14+ charge state (*m/z* 3641), along with 15+ (*m/z* 3398) and 13+ (*m/z* 3921), giving a MW of 50,960 Da. Ubiquitin carboxyl-terminal hydrolase showed a major 10+ charge state (*m/z* 2780), with 11+ (*m/z* 2527) and 9+ (*m/z* 3089), corresponding to a MW of 27,792 Da. The HU homolog displayed a dominant 12+ charge state (*m/z* 2901), along with 13+ (*m/z* 2678) and 11+ (*m/z* 3170), corresponding to a MW of 34,803 Da. Lastly, the ubiquitin-conjugating enzyme showed a major 9+ charge state (*m/z* 1953), consistent with a calculated MW of 17,570 Da.

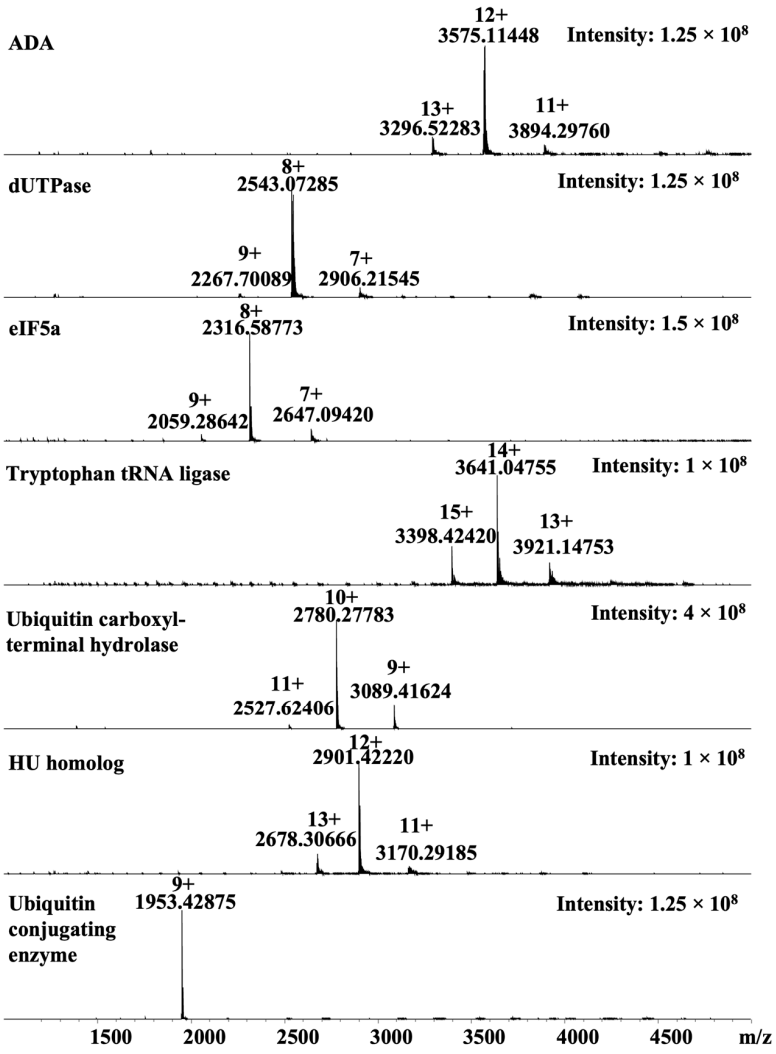


Figure 1. Native MS spectra of seven malarial proteins, each analyzed individually at 10 μM.

The *m/z* values of all seven proteins ranged from 1900 to 3900, with the closest signals observed for ADA and tryptophan tRNA ligase at *m/z* 3575 and 3641, respectively. This narrow *m/z* distribution suggests that these proteins can be analyzed simultaneously in a mixed-protein native MS experiment without significant spectral overlap. To evaluate this, the seven proteins were combined and subjected to native MS analysis. The previous study has shown that protein signal intensities in mixed samples can be strongly influenced by both the concentration and pH of the ammonium acetate buffer, as well as by MS instrument parameters [35]. Based on these findings, and to maintain a physiologically relevant pH around 7.3, we focused on optimizing buffer concentration while keeping the pH constant. A total of four ammonium acetate concentrations, 10 mM, 50 mM, 100 mM, and 200 mM, were evaluated for their effect on the spectral quality of the protein mixture.

Across the four tested buffer concentrations, signal intensities for the seven malarial proteins demonstrated notable variation, reflecting both buffer-dependent and protein-specific differences in ionization efficiency (Figure 2). The protein dUTPase exhibited its strongest signal at 10 mM, with intensities sharply decreasing at 50 mM and further at 100 mM, suggesting a preference for lower ionic strength. The HU homolog showed a similar trend of gradual signal reduction with increasing buffer concentration, indicating sensitivity to higher ionic strength. In contrast, the ubiquitin-conjugating enzyme maintained consistently high intensities across all four concentrations, with a slight increase at 50 mM buffer, indicating robustness to buffer conditions. Notably, both eIF5A and ubiquitin carboxyl-terminal hydrolase showed a clear preference for 50 mM buffer, with their signal intensities dramatically decreasing under the other three tested conditions.

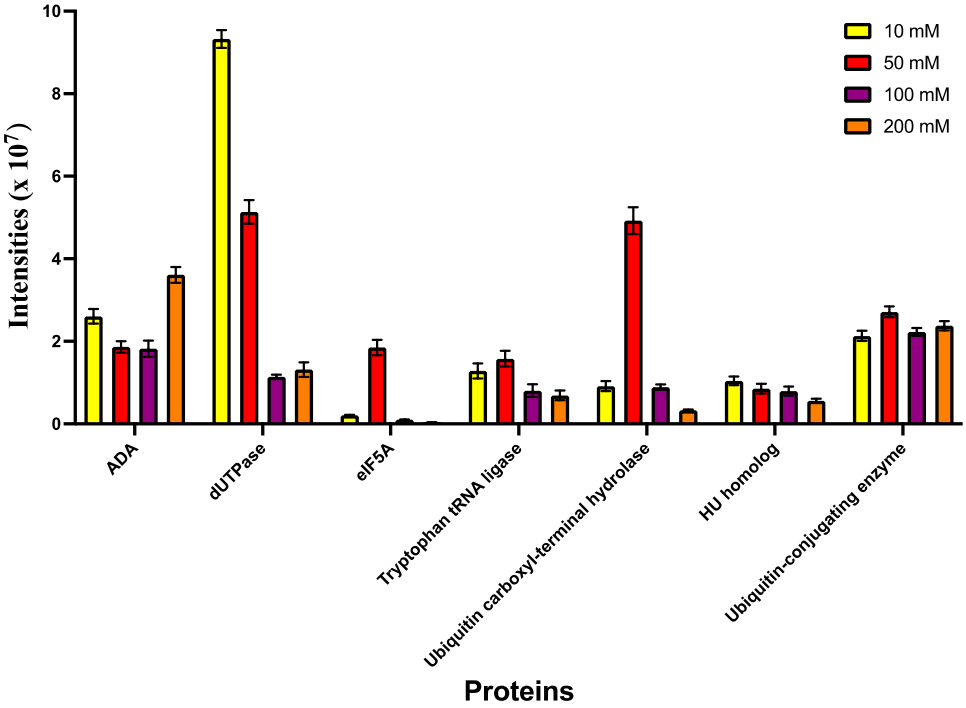


Figure 2. Native MS protein signal intensities of the protein mixture (each protein at 5 μM) under different ammonium acetate concentrations. Measurements were performed in triplicate.

Interestingly, despite a general decrease in total signal intensity for most proteins at 200 mM buffer, ADA exhibited its highest signal under this condition, suggesting that high ionic strength may enhance ionization efficiency for certain proteins. However, this came at the cost of reduced visibility for others, such as eIF5A and ubiquitin carboxyl-terminal hydrolase. Taken together, while individual proteins responded differently to buffer concentration, 50 mM ammonium acetate emerged as the most balanced condition,

supporting strong and consistent detection across the full protein mixture. This concentration was therefore selected for simultaneous native MS analysis of the seven malarial proteins (Figure 3A).

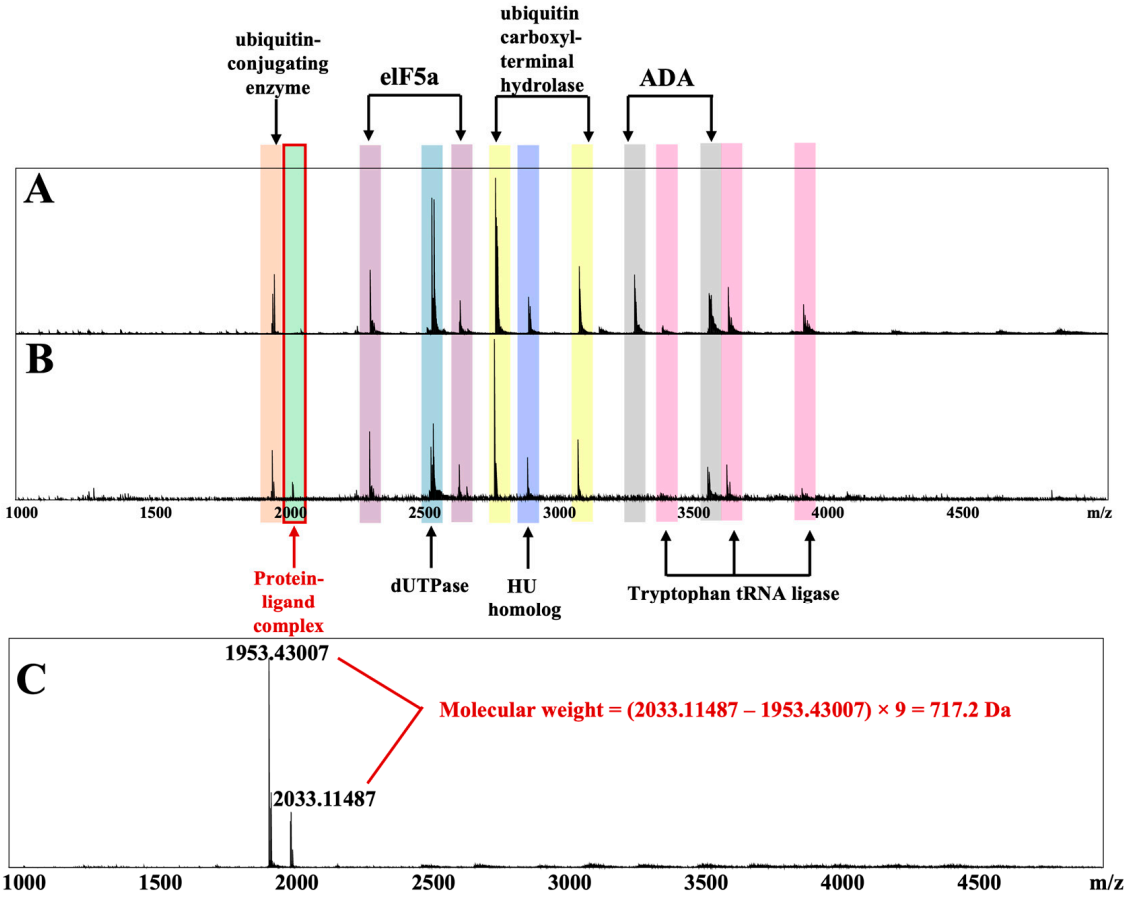


Figure 3. Native MS spectra of the seven-protein mixture (each at 5 μM) without (**A**) and with (**B**) the Danshen crude extract (1 mg/mL). Signals corresponding to each protein are color-coded. An additional peak appearing upon the addition of the extract in (**B**) is highlighted. (**C**) Native MS spectrum of the ubiquitin-conjugating enzyme (10 μM) incubated with the Danshen extract (1 mg/mL). The molecular weight of the bound ligand was calculated to be 717.2 Da.

3.3. Native MS Screening

To evaluate the applicability of the screening strategy, six ethanolic extracts derived from traditional Chinese medicines (TCMs) were tested against the seven-protein mixture. The selected TCMs, *Astragalus mongholicus* (Huangqi), *Salvia miltiorrhiza* (Danshen), *Schisandra chinensis* (Wuweizi), *Stemona tuberosa* (Baibu), *Asparagus cochinchinensis* (Tiandong), and *Cirsium japonicum* (Daji), were chosen for their reported richness in diverse secondary metabolites and their various biological activities and potential in antimalarial applications.

Native MS experiments were conducted using the seven-protein mixture (each at 5 μM), incubated individually with each TCM extract (1 mg/mL). Although a general reduction in signal intensity was observed upon addition of the crude extracts compared to the protein-only control, distinct signals corresponding to all seven proteins remained detectable. Among them, the two largest proteins, ADA and tryptophan tRNA ligase, exhibited the most pronounced signal suppression (Figure 3B).

Notably, an additional peak at *m/z* 2033.11492 was observed in the Danshen-treated sample. Its isotope distribution indicated a 9+ charge state. Given that the only protein in the mixture with a lower *m/z* than this peak was the ubiquitin-conjugating enzyme (*m/z* 1953.43017, 9+), the new signal likely corresponds to a ligand bound to this protein.

This interaction was subsequently confirmed in a separate validation experiment using the ubiquitin-conjugating enzyme incubated with the Danshen extract, where the same protein–ligand complex was observed (Figure 3C). The estimated mass of the ligand was calculated as (2033.11487 − 1953.43007) × 9 = 717.2 Da.

3.4. Ligand Purification, Identification, and Evaluation

Guided by the calculated molecular weight of the ligand, the compound was rapidly isolated using chromatographic techniques. Comparison of the nuclear magnetic resonance (NMR) (Figures S1–S5, Table S1), high-resolution MS (Figure S6), and optical rotation data with reported values [36,37] confirmed the structure of the isolated compound as lithospermate B (Figure 4A), a known polyphenolic compound previously reported from *Salvia miltiorrhiza* (Danshen) [38]. This compound is characterized by a caffeic acid tetramer structure with multiple carboxylic acid and hydroxyl groups, contributing to its high polarity and strong metal-chelating and antioxidant properties [39]. It has been extensively studied for its cardiovascular and anti-inflammatory effects [40], and its identification here highlights its previously unreported potential interaction with the ubiquitin-conjugating enzyme in a malarial context.

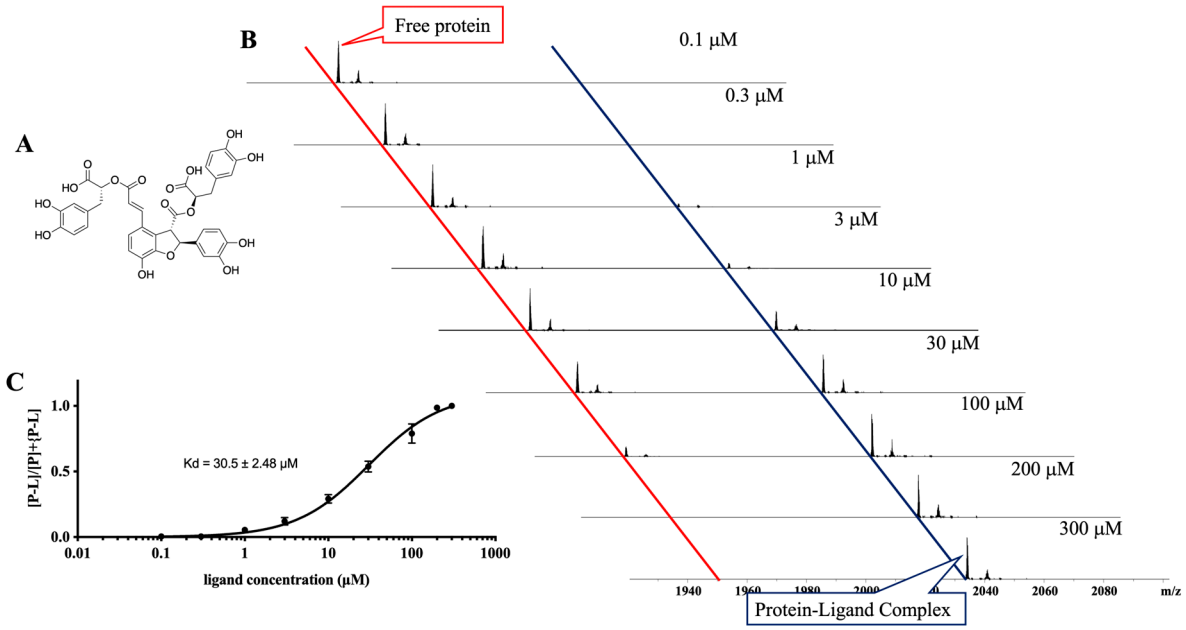


Figure 4. (**A**). Chemical structure of lithospermate B. (**B**) Overlay of the 9 mass spectra of the ubiquitin-conjugating enzyme at a concentration of 5 μM mixed with increasing concentrations of pure lithospermate B (0.1−300 μM). (**C**) Plot of [P-L]/[P] + [P-L] versus ligand concentrations for the titration of ubiquitin-conjugating enzyme with lithospermate B. The Kd was calculated as 30.55 ± 2.48 μM. The experiment was performed in triplicate.

A titration experiment was performed to evaluate the binding affinity between lithospermate B and the ubiquitin-conjugating enzyme. The protein concentration was held constant at 10 μM, while the concentration of lithospermate B was gradually increased from 0.1 μM to 300 μM until saturation of protein binding was observed. The ratio of the intensity of the protein–ligand complex peak to the total intensity (sum of the free protein peak and the protein–ligand complex peak) was plotted against the concentration of lithospermate B (Figure 4B). Using these data and Equations (1) and (2), the binding affinity Kd, defined as the ligand concentration corresponding to 50% protein binding, was determined to be 30.5 ± 2.48 μM for lithospermate B binding to the ubiquitin-conjugating enzyme (Figure 4C).

4. Discussion

Infectious diseases such as malaria continue to pose a serious global health challenge, with the rapid emergence of drug-resistant strains demanding the development of innovative therapeutic strategies. Native MS has already established itself as a powerful, label-free technique capable of preserving non-covalent interactions and providing direct mass readouts for protein–ligand complexes. However, its application has typically been confined to one protein target at a time. In this study, we report an advancement of native MS as a screening platform capable of simultaneously analyzing protein–ligand interactions across multiple protein targets in a single experiment.

The platform represents a notable step forward by demonstrating the feasibility of analyzing protein–ligand interactions in a seven-protein multiplexed format. This was achieved by the careful optimization of the buffer conditions (e.g., 50 mM ammonium acetate at pH 7.3), allowing consistent detection of all proteins in the mixture while maintaining sensitivity to ligand binding. While spectral overlap is a potential concern in multi-protein analysis, our results show that proteins with non-overlapping *m/z* distributions can be effectively distinguished, even in the presence of complex ligand mixtures.

The utility of this platform was validated using crude extracts from TCMs. Despite general signal suppression due to extract complexity, clear protein–ligand binding events remained detectable. Notably, a ligand lithospermate B with a molecular weight of 718 Da was identified from *Salvia miltiorrhiza* (Danshen) as specifically binding to the ubiquitin-conjugating enzyme and confirmed to bind with moderate affinity (Kd = 30.5 ± 2.5 μM) using a titration-based native MS binding assay.

Although no previous studies have reported natural products binding to malarial ubiquitin-conjugating enzymes, several natural products have been identified to interact with E2 enzymes in other organisms [41]. For example, leucettamol A inhibited the Ubc13–Uev1A interaction with an IC_{50} of 106 μM [42], while its fully hydrogenated derivative showed improved potency with an IC_{50} of 8 μM [43]. Moreover, manadosterols A and B exhibited even stronger inhibition with IC_{50} values of 0.09 and 0.13 μM, respectively [44]. Variabine B also inhibited Ubc13–Uev1A interaction with IC_{50} values between 16 and 20 μM [45]. Compared to these values, the Kd of lithospermate B binding to the malarial ubiquitin-conjugating enzyme (30.5 ± 2.5 μM) falls within the moderate affinity range, suggesting that lithospermate B represents a promising starting point for further optimization.

Looking forward, further developments could include the expansion of the protein panel beyond seven targets, the integration with automated sample handling, and the use of ion mobility MS for improved resolution of overlapping species. From a drug discovery perspective, this platform may be particularly impactful for natural product-based screening, phenotypic deconvolution, and target identification, where speed, sensitivity, and the ability to work with complex mixtures are crucial.

In conclusion, the multiplexed native MS screening platform described here to simultaneously screen multiple targets expands the throughput and information content of early-stage drug discovery. By enabling simultaneous detection of protein–ligand interactions across multiple targets with minimal sample preparation, it represents a powerful addition to the drug discovery toolbox, with broad applications in both infectious disease research and beyond.

Supplementary Materials: The following supporting information can be downloaded at: https://www.mdpi.com/article/10.3390/chemosensors13050166/s1, Figure S1. ^{1}H NMR spectrum (800 MHz) of lithospermate B measured in DMSO-d_6. Figure S2. ^{13}C NMR spectrum (200 MHz) of lithospermate B measured in DMSO-d_6. Figure S3. COSY spectrum of lithospermate B measured in DMSO-d_6.

Figure S4. HSQC spectrum of lithospermate B measured in DMSO-d_6. Figure S5. HMBC spectrum of lithospermate B measured in DMSO-d_6. Figure S6. HRMS spectrum of lithospermate B. Table S1. NMR data comparison for lithospermate B. Reference [37] is cited in the Supplementary Materials.

Author Contributions: Conceptualization, M.L.; methodology, J.H. and M.L.; data collection, J.H. and M.L.; writing—original draft preparation, J.H. and M.L.; writing—review and editing, J.H., W.C.V.V., R.J.Q. and M.L.; funding acquisition, M.L. All authors have read and agreed to the published version of the manuscript.

Funding: This research was funded by the 2019 Griffith Institute for Drug Discovery Early Career Researcher Grant (Griffith Institute for Drug Discovery, ESK2681) and the 2020 Griffith Sciences New Researcher Grant (Griffith Sciences, ESK2551). M.L. is supported by a National Health and Medical Research Council (NHMRC) Investigator Grant (NHMRC, INV2017517).

Institutional Review Board Statement: Not applicable.

Informed Consent Statement: Not applicable.

Data Availability Statement: Data are contained within the article and Supplementary Materials.

Conflicts of Interest: The authors declare no conflicts of interest.

References

1. *World Malaria Report 2024*; World Health Organization: Geneva, Switzerland, 2024; pp. 1–50.
2. Duffey, M.; Shafer, R.W.; Timm, J.; Burrows, J.N.; Fotouhi, N.; Cockett, M.; Leroy, D. Combating Antimicrobial Resistance in Malaria, HIV and Tuberculosis. *Nat. Rev. Drug Discov.* **2024**, *23*, 461–479. [CrossRef]
3. Turschner, S.; Efferth, T. Drug Resistance in Plasmodium: Natural Products in the Fight Against Malaria. *Mini-Rev. Med. Chem.* **2009**, *9*, 206–214. [CrossRef] [PubMed]
4. Tamara, S.; den Boer, M.A.; Heck, A.J.R. High-Resolution Native Mass Spectrometry. *Chem. Rev.* **2022**, *122*, 7269–7326. [CrossRef] [PubMed]
5. O'Connell, N. Protein Ligand Interactions Using Surface Plasmon Resonance. *Methods Mol. Biol.* **2021**, *2365*, 3–20. [PubMed]
6. Damian, L. Isothermal Titration Calorimetry for Studying Protein-Ligand Interactions. *Methods Mol. Biol.* **2013**, *1008*, 103–118.
7. Groftehauge, M.K.; Hajizadeh, N.R.; Swann, M.J.; Pohl, E. Protein-ligand interactions investigated by thermal shift assays (TSA) and dual polarization interferometry (DPI). *Acta Crystallogr. D* **2015**, *71*, 36–44. [CrossRef]
8. Leney, A.C.; Heck, A.J. Native Mass Spectrometry: What is in the Name? *J. Am. Soc. Mass Spectrom.* **2017**, *28*, 5–13. [CrossRef]
9. Bennett, J.L.; Nguyen, G.T.H.; Donald, W.A. Protein-Small Molecule Interactions in Native Mass Spectrometry. *Chem. Rev.* **2022**, *122*, 7327–7385. [CrossRef]
10. Barth, M.; Schmidt, C. Native Mass Spectrometry-A Valuable Tool in Structural Biology. *J. Mass Spectrom.* **2020**, *55*, e4578. [CrossRef]
11. Fiorentino, F.; Rotili, D.; Mai, A. Native Mass Spectrometry-directed Drug Discovery: Recent Advances in Investigating Protein Function and Modulation. *Drug Discov. Today* **2023**, *28*, 103548. [CrossRef]
12. Gavriilidou, A.F.M.; Sokratous, K.; Yen, H.Y.; De Colibus, L. High-Throughput Native Mass Spectrometry Screening in Drug Discovery. *Front. Mol. Biosci.* **2022**, *9*, 837901. [CrossRef]
13. Gu, Y.S.; Liu, M.M.; Staker, B.L.; Buchko, G.W.; Quinn, R.J. Drug-Repurposing Screening Identifies a Gallic Acid Binding Site on SARS-CoV-2 Non-structural Protein 7. *ACS Pharmacol. Transl.* **2023**, *6*, 578–586. [CrossRef] [PubMed]
14. Quinn, R.J.; Mak, T.; Littler, D.R.; Rossjohn, J.; Liu, M.M. Discovery of Anti-SARS-CoV-2 Nsp9 Binders from Natural Products by a Native Mass Spectrometry Approach. *J. Nat. Prod.* **2023**, *86*, 2630–2637. [CrossRef]
15. Vu, H.; Pedro, L.; Mak, T.; McCormick, B.; Rowley, J.; Liu, M.M.; Di Capua, A.; Williams-Noonan, B.; Pham, N.B.; Pouwer, R.; et al. Fragment-based Screening of a Natural Product Library against 62 Potential Malaria Drug Targets Employing Native Mass Spectrometry. *ACS Infect. Dis.* **2018**, *4*, 431–444. [CrossRef] [PubMed]
16. Vu, H.; Roullier, C.; Campitelli, M.; Trenholme, K.R.; Gardiner, D.L.; Andrews, K.T.; Skinner-Adams, T.; Crowther, G.J.; Van Voorhis, W.C.; Quinn, R.J. Gametocyte Inhibition Identified from a Natural-Product-Based Fragment Library. *ACS Chem. Biol.* **2013**, *8*, 2654–2659. [CrossRef] [PubMed]
17. Elnaas, A.R.; Grice, D.; Han, J.Y.; Feng, Y.J.; Capua, A.D.; Mak, T.; Laureanti, J.A.; Buchko, G.W.; Myler, P.J.; Cook, G.; et al. Discovery of a Natural Product That Binds to the Mycobacterium tuberculosis Protein Rv1466 Using Native Mass Spectrometry. *Molecules* **2020**, *25*, 2384. [CrossRef]

18. Bajsa, J.; McCluskey, A.; Gordon, C.P.; Stewart, S.G.; Hill, T.A.; Sahu, R.; Duke, S.O.; Tekwani, B.L. The Antiplasmodial Activity of Norcantharidin Analogs. *Bioorg. Med. Chem. Lett.* **2010**, *20*, 6688–6695. [CrossRef]
19. Suberu, J.O.; Gorka, A.P.; Jacobs, L.; Roepe, P.D.; Sullivan, N.; Barker, G.C.; Lapkin, A.A. Anti-Plasmodial Polyvalent Interactions in Artemisia annua L. Aqueous Extract-Possible Synergistic and Resistance Mechanisms. *PLoS ONE* **2013**, *8*, e80790. [CrossRef]
20. Cui, M.; Du, Y. Native Mass Spectrometry for Characterization of Proteins Binding with Small Molecules and Application in Drug Discovery. *TrAC-Trend Anal. Chem.* **2024**, *174*, 117701. [CrossRef]
21. Jaruwat, A.; Riangrungroj, P.; Ubonprasert, S.; Sae-ueng, U.; Kuaprasert, B.; Yuthavong, Y.; Leartsakulpanich, U.; Chitnumsub, P. Crystal Structure of Adenosine Deaminase Reveals a Novel Binding Pocket for Inosine. *Arch. Biochem. Biophys.* **2019**, *667*, 6–13. [CrossRef]
22. Tyler, P.C.; Taylor, E.A.; Fröhlich, R.F.G.; Schramm, V.L. Synthesis of 5′-methylthio Coformycins: Specific Inhibitors for Malarial Adenosine Deaminase. *J. Am. Chem. Soc.* **2007**, *129*, 6872–6879. [CrossRef]
23. Whittingham, J.L.; Leal, I.; Nguyen, C.; Kasinathan, G.; Bell, E.; Jones, A.F.; Berry, C.; Benito, A.; Turkenburg, J.P.; Dodson, E.J.; et al. dUTPase as a Platform for Antimalarial Drug Design: Structural Basis for the Selectivity of a Class of Nucleoside Inhibitors. *Structure* **2005**, *13*, 329–338. [CrossRef] [PubMed]
24. Pérez-Moreno, G.; Sánchez-Carrasco, P.; Ruiz-Pérez, L.M.; Johansson, N.G.; Müller, S.; Baragana, B.; Hampton, S.E.; Gilbert, I.H.; Kaiser, M.; Sarkar, S.; et al. Validation of dUTPase as the Target of 5′-tritylated Deoxyuridine Analogues with Anti-malarial Activity. *Malaria J.* **2019**, *18*, 392. [CrossRef]
25. Baragaña, B.; McCarthy, O.; Sánchez, P.; Bosch-Navarrete, C.; Kaiser, M.; Brun, R.; Whittingham, J.L.; Roberts, S.M.; Zhou, X.X.; Wilson, K.S.; et al. β-Branched Acyclic Nucleoside Analogues as Inhibitors of dUTPase. *Bioorg. Med. Chem.* **2011**, *19*, 2378–2391. [CrossRef] [PubMed]
26. Molitor, I.M.; Knöbel, S.; Dang, C.; Spielmann, T.; Alléra, A.; König, G.M. Translation Initiation Factor eIF-5A from Plasmodium falciparum. *Mol. Biochem. Parasit.* **2004**, *137*, 65–74. [CrossRef]
27. Kaiser, A.; Heiss, K.; Mueller, A.K.; Fimmers, R.; Matthes, J.; Njuguna, J.T. Inhibition of EIF-5A Prevents Apoptosis in Human Cardiomyocytes after Malaria Infection. *Amino Acids* **2020**, *52*, 693–710. [CrossRef] [PubMed]
28. Chhibber-Goel, J.; Yogavel, M.; Sharma, A. Structural Analyses of the Malaria Parasite Aminoacyl-tRNA Synthetases Provide New Avenues for Antimalarial Drug Discovery. *Protein Sci.* **2021**, *30*, 1793–1803. [CrossRef]
29. Pasaje, C.F.A.; Cheung, V.; Kennedy, K.; Lim, E.E.; Baell, J.B.; Griffin, M.D.W.; Ralph, S.A. Selective Inhibition of Apicoplast Tryptophanyl-tRNA Synthetase Causes Delayed Death in *Plasmodium falciparum*. *Sci. Rep.* **2016**, *6*, 27531. [CrossRef]
30. Gonçalves, A.F.; Lima-Pinheiro, A.; Ferreira, P.E. Ubiquitin-proteasome System in Plasmodium: A Potential Antimalarial Target to Overcome Resistance-A Systematic Review. *Front. Med.* **2024**, *11*, 1441352. [CrossRef]
31. Jain, J.; Jain, S.K.; Walker, L.A.; Tekwani, B.L. Inhibitors of Ubiquitin E3 Ligase as Potential New Antimalarial Drug Leads. *BMC Pharmacol. Toxicol.* **2017**, *18*, 40. [CrossRef]
32. Imhoff, R.D.; Rosenthal, M.R.; Ashraf, K.; Bhanot, P.; Ng, C.L.; Flaherty, D.P. Identification of Covalent Fragment Inhibitors for Plasmodium falciparum UCHL3 with Anti-malarial Efficacy. *Bioorg. Med. Chem. Lett.* **2023**, *94*, 129458. [CrossRef]
33. Sasaki, N.; Hirai, M.; Maeda, K.; Yui, R.; Itoh, K.; Namiki, S.; Morita, T.; Hata, M.; Murakami-Murofushi, K.; Matsuoka, H.; et al. The Plasmodium HU Homolog, Which Binds the Plastid DNA Sequence-independent Manner, Is Essential for the Parasite's Survival. *Febs Lett.* **2009**, *583*, 1446–1450. [CrossRef] [PubMed]
34. Nguyen, G.T.H.; Bennett, J.L.; Liu, S.; Hancock, S.E.; Winter, D.L.; Glover, D.J.; Donald, W.A. Multiplexed Screening of Thousands of Natural Products for Protein-Ligand Binding in Native Mass Spectrometry. *J. Am. Chem. Soc.* **2021**, *143*, 21379–21387. [CrossRef] [PubMed]
35. Liu, M.; Van Voorhis, W.C.; Quinn, R.J. Development of a Target Identification Approach Using Native Mass Spectrometry. *Sci. Rep.* **2021**, *11*, 2387. [CrossRef]
36. Jung, M.; Lee, H.C.; Ahn, C.W.; Park, W.; Choi, S.; Kim, H.; Cho, D.; Lee, G.T.; Li, H.R. Effective Isolation ofMmagnesium Lithospermate B and Its Inhibition of Aldose Reductase and Fibronectin on Mesangial Cell Line. *Chem. Pharm. Bull.* **2002**, *50*, 1135–1136. [CrossRef] [PubMed]
37. Xuan, L.J.; Wang, Y.P.; Song, W.B.; Chen, C.G.; Li, D.X.; Zhou, X.Y.; Gu, Y.L.; Hu, L.; Zhao, J.; Xu, W.W.; et al. High-Purity Magnesium Lithospermat B and Preparation Method Therefor. European Patent No. EP3127905, 9 February 2015. Available online: https://patentscope.wipo.int/search/en/detail.jsf?docId=EP192181374&_fid=WO2015149589 (accessed on 15 October 2024).
38. Guo, Y.X.; Shi, C.Z.; Zhang, L.; Lv, L.; Zhang, Y.Y. Extraction and Isolation of Lithospermic Acid B from Salvia miltiorrhiza Bunge Using Aqueous Two-phase Extraction Followed by High-performance Liquid Chromatography. *J. Sep. Sci.* **2016**, *39*, 3624–3630. [CrossRef]
39. Lin, N.H.; Chung, T.Y.; Li, F.Y.; Chen, H.A.; Tzen, J.T.C. Enhancing the Potency of Lithospermate B for Inhibiting Na/K-ATPase Activity by Forming Transition Metal Ion Complexes. *Acta Pharmacol. Sin.* **2013**, *34*, 893–900. [CrossRef]
40. Qu, C.; Xu, Y.; Yang, X.L.; Lu, X. Magnesium Lithospermate B Improves Pulmonary Artery Banding Induced Right Ventricular Dysfunction by Alleviating Inflammation via p38MAPK Pathway. *Pulm. Pharmacol. Ther.* **2020**, *63*, 101935. [CrossRef]

41. Hess, W.; Mackeen, M.M.; Kramer, H.B. Natural Product Inhibitors of Ubiquitin Conjugation and Deconjugation. *Stud. Nat. Prod. Chem.* **2016**, *49*, 207–242.
42. Kong, F.; Faulkner, D.J. Leucettamines A and B, Two Antimicrobial Lipids from the Calcareous Sponge *Leucetta microraphis*. *J. Org. Chem.* **1993**, *58*, 970–971. [CrossRef]
43. Tsukamoto, S.; Takeuchi, T.; Rotinsulu, H.; Mangindaan, R.E.P.; van Soest, R.W.M.; Ukai, K.; Kobayashi, H.; Namikoshi, M.; Ohta, T.; Yokosawa, H. Leucettamol A: A new inhibitor of Ubc13-Uev1A interaction isolated from a marine sponge, *Leucetta* aff. *microrhaphis*. *Bioorg. Med. Chem. Lett.* **2008**, *18*, 6319–6320. [CrossRef] [PubMed]
44. Ushiyama, S.; Umaoka, H.; Kato, H.; Suwa, Y.; Morioka, H.; Rotinsulu, H.; Losung, F.; Mangindaan, R.E.P.; de Voogd, N.J.; Yokosawa, H.; et al. Manadosterols A and B, Sulfonated Sterol Dimers Inhibiting the Ubc13-Uev1A Interaction, Isolated from the Marine Sponge. *J. Nat. Prod.* **2012**, *75*, 1495–1499. [CrossRef] [PubMed]
45. Sakai, E.; Kato, H.; Rotinsulu, H.; Losung, F.; Mangindaan, R.E.P.; de Voogd, N.J.; Yokosawa, H.; Tsukamoto, S. Variabines A and B: New β-carboline Alkaloids from the Marine Sponge. *J. Nat. Med.* **2014**, *68*, 215–219. [CrossRef] [PubMed]

Disclaimer/Publisher's Note: The statements, opinions and data contained in all publications are solely those of the individual author(s) and contributor(s) and not of MDPI and/or the editor(s). MDPI and/or the editor(s) disclaim responsibility for any injury to people or property resulting from any ideas, methods, instructions or products referred to in the content.